Late Holocene climate reorganisation and the North American Monsoon

Jones, Matthew D; Metcalfe, S. E.; Davies, Sarah Jane; Noren, Anders

Published in:
Quaternary Science Reviews

DOI:
10.1016/j.quascirev.2015.07.004

Publication date:
2015

Citation for published version (APA):
Jones, M. D., Metcalfe, S. E., Davies, S. J., & Noren, A. (2015). Late Holocene climate reorganisation and the North American Monsoon. *Quaternary Science Reviews*, *124*, 290-295. https://doi.org/10.1016/j.quascirev.2015.07.004

Late Holocene climate reorganisation and the North American Monsoon

Matthew D. Jones[1]*, Sarah E. Metcalfe[1], Sarah J. Davies[2] and Anders Noren[3]

1. School of Geography, University of Nottingham, NG7 2RD,UK (matthew.jones@nottingham.ac.uk; sarah.metcalfe@nottingham.ac.uk)
2. Department of Geography and Earth Sciences, Aberystwyth University, SY23 3DB, UK (sjd@aber.ac.uk)
3. Limnological Research Center (LRC), University of Minnesota, Minneapolis MN 55455, USA (noren021@umn.edu)

*Corresponding author: Tel: +44(0)115 8468406

Abstract

The North America Monsoon (NAM) provides the majority of rainfall for central and northern Mexico as well as parts of the south west USA. The controls over the strength of the NAM in a given year are complex, and include both Pacific and Atlantic systems. We present here an annually resolved proxy reconstruction of NAM rainfall variability over the last ~6ka, from an inwash record from the Laguna de Juanacatlán, Mexico. This high resolution, exceptionally well dated record allows changes in the NAM through the latter half of the Holocene to be investigated in both time and space domains, improving our understanding of the controls on the system. Our analysis shows a shift in conditions between c. 4 and 3 ka BP, after which clear ENSO/PDO type forcing patterns are evident.

Keywords

Mexico, North American Monsoon, Holocene, XRF scanning, ENSO, PDO, AMO

Highlights

- Annual proxy rainfall record of the late Holocene North America Monsoon
- Significant variability at ~2000, ~565, ~65 and ~22 year frequencies
- Present day North American Monsoon patterns were established after 3ka BP

1. Introduction

The North American Monsoon (NAM) is a crucial precipitation source within its core region of Mexico and the south-west USA, providing up to 60% of annual precipitation (Metcalfe et al. 2015, Fig. 3b; Ropelewski et al., 2005), and is vital to sustaining agriculture, industry and biodiversity. Climate change projections for the NAM region suggest that both increased temperatures and reduced precipitation are likely in the coming century (Karmalkar et al., 2011). Better understanding of NAM variability and its controls are therefore essential (Englehart and Douglas, 2002). High temporal resolution proxy records (e.g. Stahle et al., 2012) are necessary to identify both the long term evolution of the NAM and its variability under different climate modes.

The NAM arises from the seasonal, insolation driven, northward migration of the Intertropical Convergence Zone (ITCZ) in the Northern Hemisphere (NH) summer, the development of a thermal low over the SW USA, and the development of a strong thermal contrast off the coast of Baja California (Barron et al., 2012). Its duration and intensity are affected by conditions in both the eastern tropical Pacific and the North Atlantic (Englehart and Douglas, 2002, 2010; Mendez and Magaña, 2010). Investigations into the controlling role of the Pacific have focussed on the El Niño Southern Oscillation (ENSO) (Castro et al., 2001; Magaña et al., 2003) and the Pacific Decadal Oscillation (PDO), recognising that these are not entirely independent (Gutzler, 2004), as the PDO can be seen as an example of ENSO-type variability operating over different timescales (Castro et al., 2001; Wilson et al, 2010). In Mexico, NAM summer rainfall is reduced during El Niño events and positive phases of the Pacific Decadal Oscillation (PDO) (Castro et al., 2001; Magaña et al., 2003; Bhattacharya and Chiang, 2014) when the eastern tropical Pacific warms and the thermal gradient to the continental interior is reduced. During La Niña or negative PDO phases, summer NAM rainfall increases. NAM drivers associated with the North Atlantic, specifically the Atlantic Multidecadal Oscillation (AMO) and the North Atlantic Oscillation (NAO) (Mendez and Magaña, 2010), seem to have their greatest impact on the NAM in the summer season. Positive (warm) phases of the AMO give rise to wetter summers in central and southern

Mexico and the wider Caribbean, as the ITCZ moves north, generating more Atlantic tropical cyclones (Knight et al., 2006; Mendez and Magaña, 2010).

Understanding controls on NAM region precipitation is complicated by complex and variable connections between the two regions of NAM forcing i.e. Atlantic and Pacific Oceans (Englehart and Douglas, 2010; Stahle et al., 2012) and variability in, often localised, storm events (Curtis, 2008). It is also increasingly evident that NAM rainfall patterns are not spatially homogeneous and it has been suggested (Castro et al., 2001) that the NAM in Mexico should be treated separately from the NAM in the south-west USA, where winter rain is more significant and El Niño or positive PDO give rise to increased winter precipitation and overall wetter conditions.

Here we present an annually resolved proxy record of precipitation through the last 6000 years from the Laguna de Juanacatlán (Jalisco, Mexico) which is located close to the tropical core of the NAM (Englehart and Douglas, 2002). The record shows a marked shift in the dominant frequencies of variability between 4 and 3 cal ka BP. This change in the frequency domain coincides with a general shift in conditions through this time period to the pattern of precipitation seen today.

2. Site Description

Laguna de Juanacatlán (20°37′N, 104°44′W; 2000 m.a.s.l.) is a lava-dammed lake with a maximum depth of 25–30 m, in the Sierra de Mascota close to the Pacific coast of Mexico. The basin (approximately 10 km^2) is orientated in a southeast to northwest direction, with the lake occupying about 0.5 km^2 at the northwest end (Metcalfe et al., 2010). The closest meteorological station is in Mascota (800 m lower and 12 km away) where annual average precipitation is 1026 mm/yr, of which 88% falls between June and October.

The sediments of Juanacatlán contain fine, mm scale laminations, with alternating organic, diatomaceous layers and pink clay from catchment in-wash. In addition a number of thick, cm scale, fining up layers consisting of sands and clays are present, which are interpreted as instantaneous turbidites.

Titanium (Ti) has been shown, via XRF scanning (see methods below), to mark the pink clay layers in the core and through comparison with observational, instrumental and historical records and other regional rainfall proxies through the last 2000 years, has been established as a proxy for run-off, which is derived principally from summer rainfall in this catchment (Metcalfe et al., 2010). The Ti profile from high resolution XRF scanning has been shown to follow sedimentary changes, recording higher values in the pink clay layers.

3. Methods and results

Two parallel, continuous cores (both ca. 9 m long) were taken from the deepest part of Laguna de Juanacatlán using a Kullenberg coring system, resulting, once disturbed sections of core had been avoided and instantaneous turbidites excluded from the record, in a 7.25m continuous composite core sequence.

27 AMS radiocarbon age estimates from bulk organic matter were obtained from the core sequence, including two dates from sediment trap and core-top material to check for any reservoir effect (Fig. 1; Supplementary Table 1). Additional age control for the top of the core is supplied by clear peaks in ^{137}Cs (Metcalfe et al., 2010).

U-channels (2cm wide) were taken from the cores and scanned using an ITRAX XRF scanner at 200 μm resolution (Croudace et al., 2006). An annually resolved Ti record was produced from the original 200 μm data set between 50 and 5821 years BP; each 200 μm data point was given an age from the age-depth model and then rounded to the nearest year. Annual values were then calculated as the mean value for all the data points rounded to that given year.

The resulting record of rainfall variability (Fig. 2) shows variation at all time scales from inter-annual to millennial through the last 6000 years. Wavelet analysis of the Ti record identified variation at different frequencies (Fig. 2); significant (95% confidence interval) cycles appear at ~2000, ~565, ~105 and ~65 and ~22 years through large parts of the record (Fig. 3).

4. Discussion

The striking feature of the Juanacatlán Ti record is the change between 3 and 4 cal ka BP that marks a shift in the dominant frequencies of variability (Fig. 3). This period, particularly between 2.8 and 3.8 cal ka BP, is also a time during which overall precipitation apparently reduced (Fig. 2a), recording the lowest average Ti values for any individual 1000 year period in the record. Frequencies similar to the significant multi-centennial and millennial frequencies (~565 and ~2000 years) found in the Juanacatlán record, which both increase notably in strength after 3ka BP, have been observed elsewhere regionally in the Gulf of Mexico (Poore et al., 2004) and Chihuahua, northern Mexico (Castiglia and Fawcett, 2006) as well as in Lake Pallcacocha, Ecuador (Moy et al., 2002; Fig. 4). Interestingly, the ~200 year cycle, reported from other parts of the NAM region and often associated with solar activity (e.g. Jimenez-Moreno et al., 2008), is not evident here.

The Juanacatlán record has comparative cycles to the Pallcacocha red intensity record (Fig. 4); the two are out of phase in the 2000 yr cycle, with periods of increased rainfall at Juanacatlán associated with reduced rainfall periods at Pallcacocha, as would be expected from a modern day ENSO type forcing. The millennial periods of enhanced NAM rainfall at Juanacatlán, which increase in strength after 3 cal ka BP (Fig. 2 and 3), are also associated with warmer phases of the multi-millennial variability in the North Pacific Gyre (Isono et al., 2009), again consistent with ENSO/PDO type forcing patterns. Carre et al. (2014), Cobb et al. (2013), and Koutavas and Joanides (2012) have also all show an increase in ENSO variance at around 3 cal ka BP.

Further evidence of the links between rainfall at Juanacatlán and Pacific forcing post 3 cal ka BP comes from a comparison of the Juanacatlán Ti record with a tree ring PDO reconstruction (MacDonald and Case, 2005) over the last millennium (Fig. 5), showing similarity in significant periodicities at centennial time scales, and to a lesser extent at 26 and 40 years (Fig. 5). These periodicities are rarely dominant at Juanacatlán prior to 4 cal ka BP, but do become more important after 3 cal ka BP. The period of most persistent positive PDO

values, AD 1400 – 1600 was marked by a dry phase at Juanacatlán (Fig. 5), again consistent with Pacific, ENSO type, forcing of the NAM.

Spatial variability in change through the 4-3 cal ka BP transition also points to a Pacific forcing of regional precipitation. Plotting changes over this period across the wider tropical Americas (Fig. 6) reveals substantial evidence for drying in the present day summer rainfall region of the North American Tropics (NAT). Together with cooling in the Gulf of Mexico and the onset of wetter conditions in the southern hemisphere summer rainfall zone, this is consistent with the southward migration of the ITCZ during the later Holocene (Haug et al., 2001) and the onset of more variable conditions (Lozano-Garcia et al., 2013; Metcalfe et al., 2015), a pattern also observed in other monsoon systems (McRobie et al., 2015). At the same time, records from the northern margin of the NAM region (where winter precipitation is more important) also indicate a shift to wetter conditions, which has been attributed to stronger ENSO or ENSO-type variability, including the PDO (Barron and Anderson, 2011).

However, both the PDO (Minobe, 1999) and the AMO (Gray et al., 2004) are potential drivers of the 60-70 year multi-decadal variability which is more important at Juanacatlán prior to 4 cal ka BP. The AMO is increasingly invoked as a driver of change in the predominantly summer rainfall regions of the NH tropical Americas (Stahle et al., 2012) and also the SW USA (Oglesby et al., 2012). Both the persistence of the AMO over most of the Holocene and its global signature have been emphasised (Knudsen et al., 2011; Wyatt et al., 2012). A similar pattern of reduced multidecadal variability, between 3.5 and 4.5 cal ka BP, followed by increased significance of bidecadal cyclicity in the late Holocene has been observed in the Pacific Northwest (Stone and Fritz, 2006), raising the possibility that the change in dominant multi decadal frequency is linked to changes in PDO frequency, rather than a link to more dominant Atlantic forcing. Insufficient data are currently available to fully resolve this issue although Bernal et al. (2011) interpret a shift in $\delta^{18}O$ at 4.3 ka in the Cueva del Diablo in southwest Mexico as marking a decoupling of local moisture from North Atlantic events to a more Pacific controlled precipitation regime.

It has been suggested that the last 6000 years may be marked by a change in overall variability in the climate system brought about by a shift from external to internal forcing (Wanner, et al., 2008; Debret et al., 2009). Despite some correlation through parts of the last 1000 years (Metcalfe et al., 2010), there is no clear relationship between solar variability and the 6000 year record from Juanacatlán (Supplementary Figure), which is consistent with the lack of a 200 year solar cycle (see discussion above), and of a dominantly internal forcing regime for this longer time period. Evidence for a significant climate shift around 4 cal ka BP has been identified across the tropics and sub-tropics (e.g. Liu and Feng, 2012; Ponton et al., 2012), with drier conditions in the northern hemisphere and wetter conditions in the southern hemisphere tropics, consistent with a southward shift in the ITCZ (Fig. 6; Abbott et al., 2003). The Juanacatlán Ti record, the first high resolution record of the NAM tropical core through this time period, shows that the period between 4 and 3 cal ka BP marks a reorganisation in climate against a background of declining NH summer insolation and a reduced seasonality of insolation. This weakening of external forcing (Donders et al., 2008) apparently provided the context for the development of strong ENSO-type forcing of the NAM. de Boer et al. (2014) have suggested a similar pattern from records in the Indian Ocean with decoupling of ENSO from the Atlantic ITCZ ~ 2,600 cal yr BP.

5. Conclusions

Given the complexity of the NAM system and uncertainty about its forcings and their internal relationships (Arias et al., 2012) high-resolution records with excellent chronological control such as the Juanacatlán sequence are vital for robust mechanistic interpretations. Our evidence points to a shift to predominantly Pacific forcing of the NAM between 4 and 3 cal ka BP, following a period where the region of dominant forcing is less clear. This shift gave rise to the present day climatic configuration of the NAM region where complex interactions of climate controls results in differential climate responses to the same forcings across Mexico and the SW United States.

Acknowledgements

We thank Doug Schnurrenberger and Mark Shapley for their work to retrieve the cores. Colleagues at UNAM and UMSNH, Mexico contributed to the costs and execution of the fieldwork. Dating was provided by NERC Radiocarbon Facilities (Allocation 1108.0305*)* and Prof A MacKenzie, SUERC East Kilbride. The University of Nottingham and Aberystwyth University provided additional funding. We thank two anonymous reviewers for their comments that helped to improve this manuscript.

References

Abbott, M. B., Wolfe, B.B., Wolfe, A.P., Seltzer, G.O., Aravena, R., Mark, B.G., Polissar, P.J., Rodbell, D.T., Rowe, H.D. and Vuille, M., 2003. Holocene paleohydrology and glacial history of the central Andes using multiproxy lake sediment studies. *Palaeogeog. Palaeoclim. Palaeoecol.* 194, 123-138.

Arias, P.A., Fu, R., Mo, K.C., 2012. Decadal variation of rainfall seasonality in the North American Monsoon region and its potential causes. *J. Clim.* 25, 4258-4274.

Barron, J.A. & Anderson, L., 2011. Enhanced Late Holocene ENSO/PDO expression along the margins of the eastern North Pacific. *Quat. Int.* 235**,** 3-12.

Barron, J.A., Metcalfe, S.E. & Addison, J.A., 2012. Response of the North American monsoon to regional changes in ocean surface temperature. *Paleoceanography* **27**, PA3206.

Bernal, J.P., Lachniet, N., McCulloch, M., Mortimer, G., Morales, P and Cienfuegos, E. 2011. A speleothem record of Holocene climate variability from southwestern Mexico. *Quaternary Research* 75, 104-113.

Bhattacharya, T. & Chiang, J.C.H., 2014. Spatial variability and mechanisms underlying El Niño-induced droughts in Mexico. *Clim. Dyn*. 43, 3309-3326.

Carré, M., Sachs, J.P., Purca, S., Schauer, A.J. Braconnot, P., Falcón, R.A., Julien, M. and Lavallée, D., 2014. Holocene history of ENSO variance and asymmetry in the eastern tropical Pacific. *Science* 345, 1045-1048.

Castiglia, P.J. & Fawcett, P.J., 2006. Large Holocene lakes and climate change in the Chihuahuan Desert. *Geology* 34**,** 113-116.

Castro, C.L., McKee, T.B. & Pielke Sr., R.A., 2001. The relationship of the North American monsoon to tropical and North Pacific sea surface temperatures as revealed by observational analysis. *J. Clim*. 14, 4449-4473.

Cobb, K.M., Westphal, N., Sayani, H.R., Watson, J.T., Di Lorenzo, E., Cheng, H., Edwards, R.L., Charles, C.D. 2013. Highly variable El Nino-Southern Oscillation throughout the Holocene. *Science* 339, 67-70.

257 Curtis, S., 2008. The Atlantic multidecadal oscillation and extreme daily precipitation over the
258 US and Mexico during the hurricane season. *Clim. Dynam.* 30, 343-351.
259 Debret, M., Sebag, D., Crosta, X., Massei, N., Petit, J-R., Chapron, E. & Bout-Roumazeilles,
260 V., 2009. Evidence from wavelet analysis for a mid-Holocene transition in global climate
261 forcing. *Quat. Sci. Revs.* 28**,** 2675-2688.
262 de Boer, E. J., Tjallingii, R., Vélez, M. I., Rijsdijk, K. F., Vlug, A., Reichart, G. J., Prendergast,
263 A.L., de Louw, P.G.B., Florens, F.B.V., Baider, C., & Hooghiemstra, H. 2014. Climate
264 variability in the SW Indian Ocean from an 8000-yr long multi-proxy record in the Mauritian
265 lowlands shows a middle to late Holocene shift from negative IOD-state to ENSO-state. *Quat.*
266 *Sci. Revs.* 86, 175-189.
267 Donders, T.H., Wagner-Cremer, F. & Visscher, H., 2008. Integration of proxy data and model
268 scenarios for the mid-Holocene onset of modern ENSO variability. *Quat. Sci. Revs.* 27**,** 571-
269 579.
270 Englehart, P.J. & Douglas, A.V., 2002. Mexico's summer rainfall patterns: an analysis of
271 regional modes and changes in their teleconnectivity. *Atmosfera* 15, 147-164..
272 Englehart P.J. and Douglas, A.V., 2010. Diagnosing warm-season rainfall variability in
273 Mexico: a classification tree approach. *Int. J. Climatol.* 30, 694-704.
274 Gray, S.T., Graumlich, L.J., Betancourt, J.L. & Pederson, G.T., 2004. A tree-ring based
275 reconstruction of the Atlantic Multidecadal Oscillation since 1567 AD. *Geophys. Res. Lett.* 31**,**
276 L12205..
277 Gutzler, D.S., 2004. An index of interannual precipitation variability in the core of the North
278 American Monsoon region. *J. Clim.* 17**,** 4473-4480.
279 Haug, G. H., Hughen, K. A., Sigman, D. M., Peterson, L. C. & Rohl, U., 2001. Southward
280 migration of the intertropical convergence zone through the Holocene. *Science* 293, 1304-
281 1308.
282 Isono, D., Yamamoto, M., Irino, T., Oba, T., Murayama, M., Nakamura, T. & Kawahata, H.,
283 2009. The 1500-year climate oscillation in the midlatitude North Pacific during the Holocene.
284 *Geology* 37, 591-594.

285 Jiménez Moreno, G., Fawcett, P.J., Anderson, R.S., 2008. Millennial- and centennial-scale
286 vegetation and climate changes during the late Pleistocene and Holocene from northern New
287 Mexico. Quat. Sci. Rev. 27, 1442-1452.
288 Karmalkar, A.V., Bradley, R.S. & Diaz, H.F., 2011. Climate change in Central America and
289 Mexico: regional climate model validation and climate change projections. *Clim. Dynam.* 36,
290 605-629.
291 Knight, J.R., Folland, C.K. & Scaife, A.A., 2006. Climate impacts of the Atlantic Multidecadal
292 Oscillation. *Geophys. Res. Lett.* 33**,** L17706.
293 Knudsen, M.F., Seidenkrantz, M.-S., Jacobsen, B.H., Kuijpers, A., 2011. Tracking the
294 Atlantic Multidecadal Oscillation through the last 8,000 years. *Nat. Commun.* 2, 178.
295 Koutavas, A. and Joanides, S. 2012. El Nino-Southern Oscilation extrema in the Holocene
296 and Last Glacial Maximum. *Paleoceanography* 27, PA4308.
297 Liu, F. & Feng, Z., 2012. A dramatic climatic transition at ~ 4000 cal yr BP and its cultural
298 responses in Chinese cultural domains. *Holocene* 22, 1181-1197.
299 Lozano-García, S., Torres-Rodríquez, E. Ortega, B., Vázquez, G. & Caballero, M., 2013.
300 Ecosystem response to climate and disturbances in western central Mexico during the late
301 Pleistocene and Holocene. *Palaeogeogr., Palaeoclimatol., Palaeoecol*., 370, 184-195.
302 MacDonald, G. M. & Case, R. A., 2006. Variations in the Pacific Decadal Oscillation over the
303 past millennium. *Geophys. Res. Lett.* 32, L08703.
304 Magaña, V., Vazquez, J.L., Perez, J.L. & Perez, J.B., 2003. Impact of El Niño on precipitation
305 in Mexico. *Geofis. Internac*. 42, 313-330.
306 Mendez, M. & Magana, V., 2010. Regional aspects of prolonged meteorological droughts
307 over Mexico and Central America. *J. Clim.* 23, 1175-1188.
308 McRobie, F. H., Stemler, T., & Wyrwoll, K. H., 2015. Transient coupling relationships of the
309 Holocene Australian monsoon. *Quat. Sci. Revs.* 121, 120-131..
310 Metcalfe, S. E., Jones, M. D., Davies, S. J., Noren, A. & MacKenzie, A., 2010. Climate
311 variability over the last two millennia in the North American Monsoon region, recorded in
312 laminated lake sediments from Laguna de Juanacatlán, Mexico. *Holocene* 20, 1195-1206.

313 Metcalfe, S.E., Barron, J.A. & Davies, S.J., 2015. The Holocene history of the North
314 American Monsoon: 'known knowns' and 'known unknowns' in understanding its spatial and
315 temporal complexity. *Quat. Sci. Revs.* 120, 1-27.
316 Minobe, S., 1999. Resonance in bidecadal and pentadecadal climate oscillations over the
317 North Pacific: Role in climatic regime shifts. *Geophys. Res. Lett.* 26, 855-858.
318 Moy, C. M., Seltzer, G. O., Rodbell, D. T. & Anderson, D. M., 2002. Variability of El
319 Niño/Southern Oscillation activity at millennial timescales during the Holocene epoch. *Nature*
320 420, 162-165.
321 Oglesby, R., Feng, S., Hu Q. & Rowe, C., 2012. The role of the Atlantic Multidecadal
322 Oscillation on medieval drought in North America: synthesizing results from proxy data and
323 climate models. *Glob. Planet. Change* 84-85**,** 56-65.
324 Ponton, C., Giosan, L., Eglinton, T.I., Fuller, D. Q., Johnson, J.E., Kumar, P. & Collett, T.S.,
325 2012. Holocene aridification of India. *Geophys. Res. Lett*. 39, L03704.
326 Poore, R.Z., Quinn, T.M. & Verardo, S., 2004. Century-scale movement of the Atlantic
327 Intertropical Convergence Zone linked to solar variability. *Geophys. Res. Lett.* 31, L12214 .
328 Ropelewski, C.F., Gutzler, D.S., Higgins, R.W., Mechoso, C.R., 2005. The North American
329 Monsoon System. In: Change, C.-P., Wang, B., Lau, N.C.G. (Eds.), The Global Monsoon
330 System: Research and Forecast, pp. 207e218. WMO Technical Document 1266, Geneva.
331 Stahle, D.W., Burnette, D.J., Villanueva Diaz, J., Heim Jr., R.R., Fye, F.K., Cerano Paredes,
332 J., Acuna Soto, R. & Cleaveland, M.K., 2012. Pacific and Atlantic influences on
333 Mesoamerican climate over the past millennium. *Clim. Dynam.* 39**,** 1431-1466.
334 Stone, J.R. & Fritz, S.C., 2006. Multidecadal drought and Holocene climate variability in the
335 Rocky Mountains. *Geology* 34**,** 409-412.
336 Torrence, C. and Campo, G.P., 1998. A Practical Guide to Wavelet Analysis. Bulletin of the
337 American Meteorological Society 79, 61-76.
338 Wanner, H., Beer, J., Butikofer, J., Crowley, T.J., Cusbasch, U., Fluckinger, J., Goosse, H.,
339 Gorsjean, M., Joos, F., Kplan, J.O., Kuttel, M., Muller, S.A., Prentice, I.C., Solomina, O.,

340 Stocker, T.F., Tarasov, P., Wagner, M., Widmann, M., 2008. Mid- to Late Holocene climate
341 change: an overview. *Quat. Sci. Revs.* 27, 1791-1828.
342 Wilson, R., Cooke, E., D'Arrigo, R., Riedwyl, N., Evans, N.M., Tudhope, A. & Allan, R., 2010.
343 Reconstructing ENSO: the influences of method, proxy data, climate forcings and
344 teleconnections. *J. Quat. Sci.* 25**,** 62-78.
345 Wyatt, M.G., Kravtsov, S. & Tsonis, A., 2012. Atlantic Multidecadal Oscillation and northern
346 hemisphere's climate variability. *Clim. Dynam.* 38**,** 929-949..
347
348

Figures

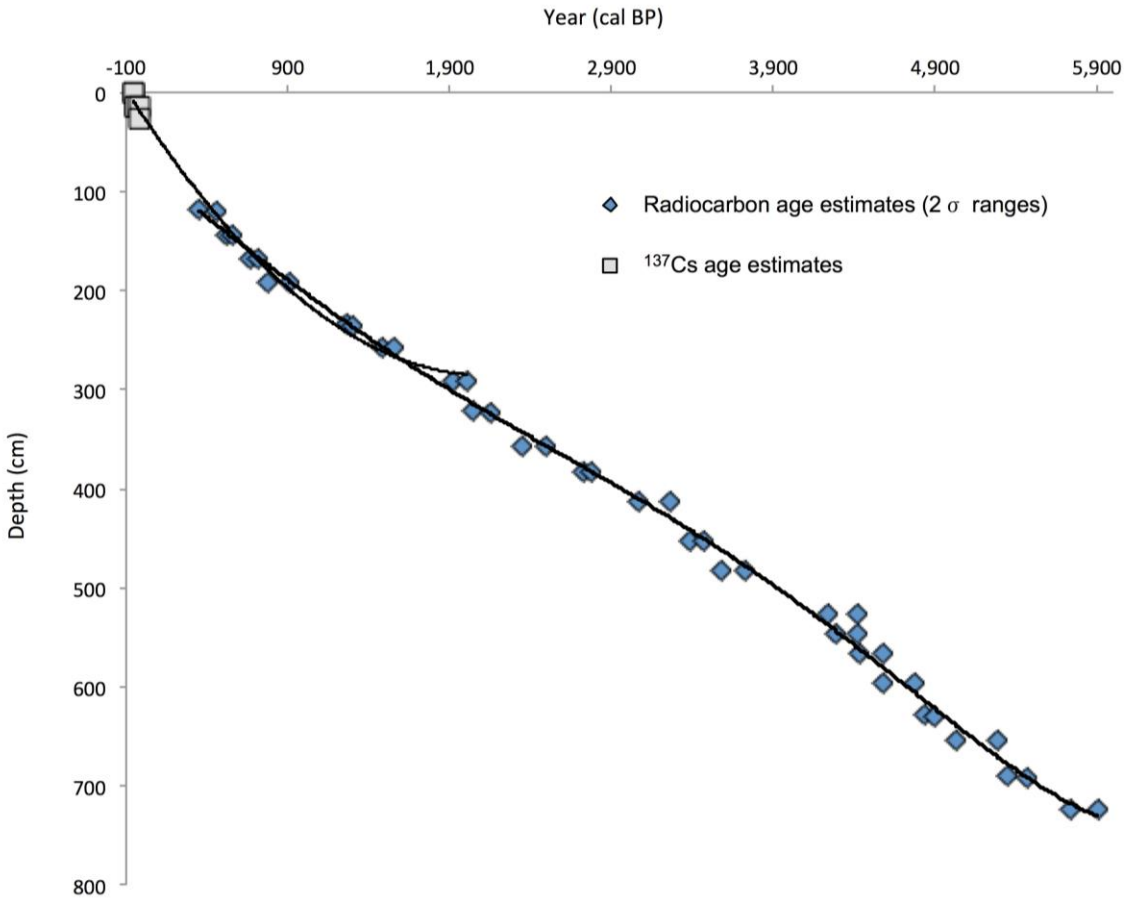

Figure 1 Age-depth model for the Juanacatlán core sequence. The model is based on a 2nd order polynomial trend at the top of the core, until 262.21 cm, and then a 5th order polynomial model through the 2 σ age ranges as shown. The full list of radiocarbon dates from the Juanacatlán sequence can be found in Supplementary Table 1.

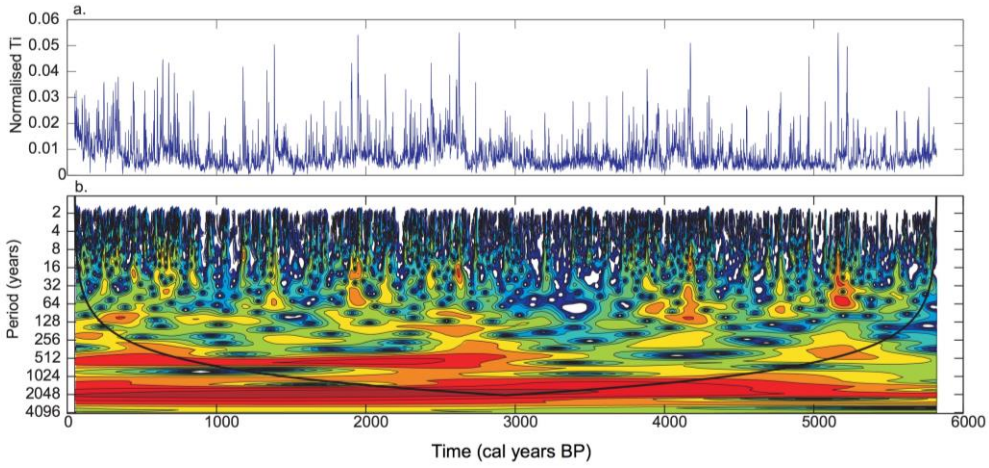

359

360

361 **Figure 2** The annual Juanacatlán Ti record (a), shown here as the Ti peak area normalised
362 to the incoherent peak area (equivalent to Compton scattering) from the XRF
363 (Supplementary Data) and a wavelet analysis of this data (b), using a Morlet wavelet in the
364 Matlab code of Torrence and Compo (1998). The time periods when the dominant
365 frequencies (red in this figure) are statistically significant are shown in Figure 3.

366

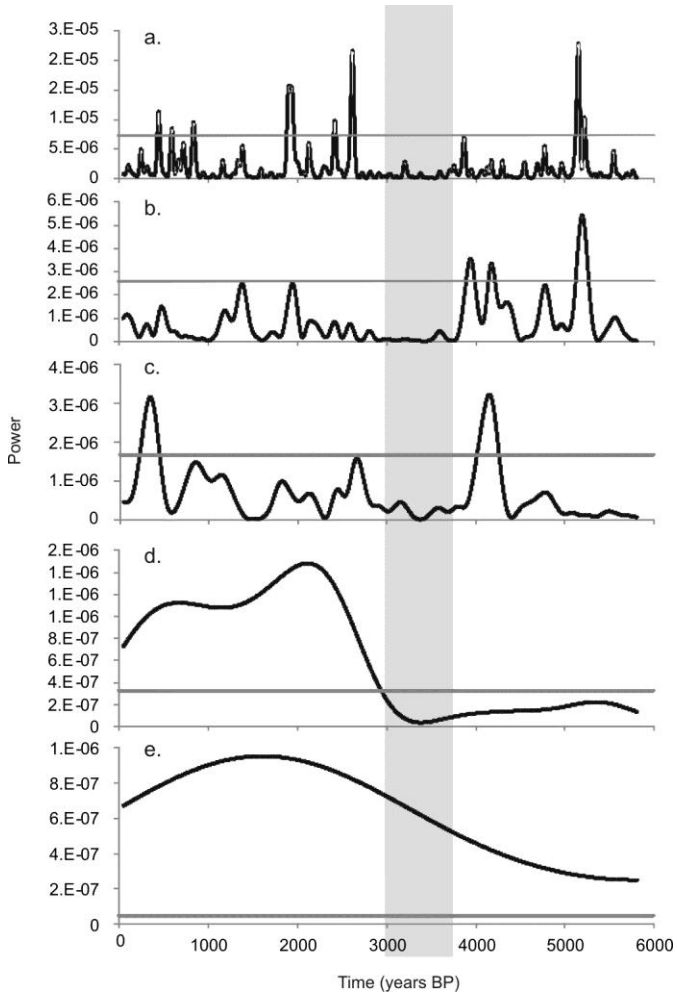

367

368 **Figure 3** Varying strength of the significant periodicities in the Juanacatlán Ti record (Fig. 2).

369 a) 20 – 25 year b) 60 – 70 years c) 100 – 115 years d) 530 – 600 years e) 1850 – 2110

370 years. Significance levels (at the 95% confidence limit) are shown by the grey lines in each

371 plot. The transitional zone between 4 and 3 cal ka BP is shaded for reference.

372

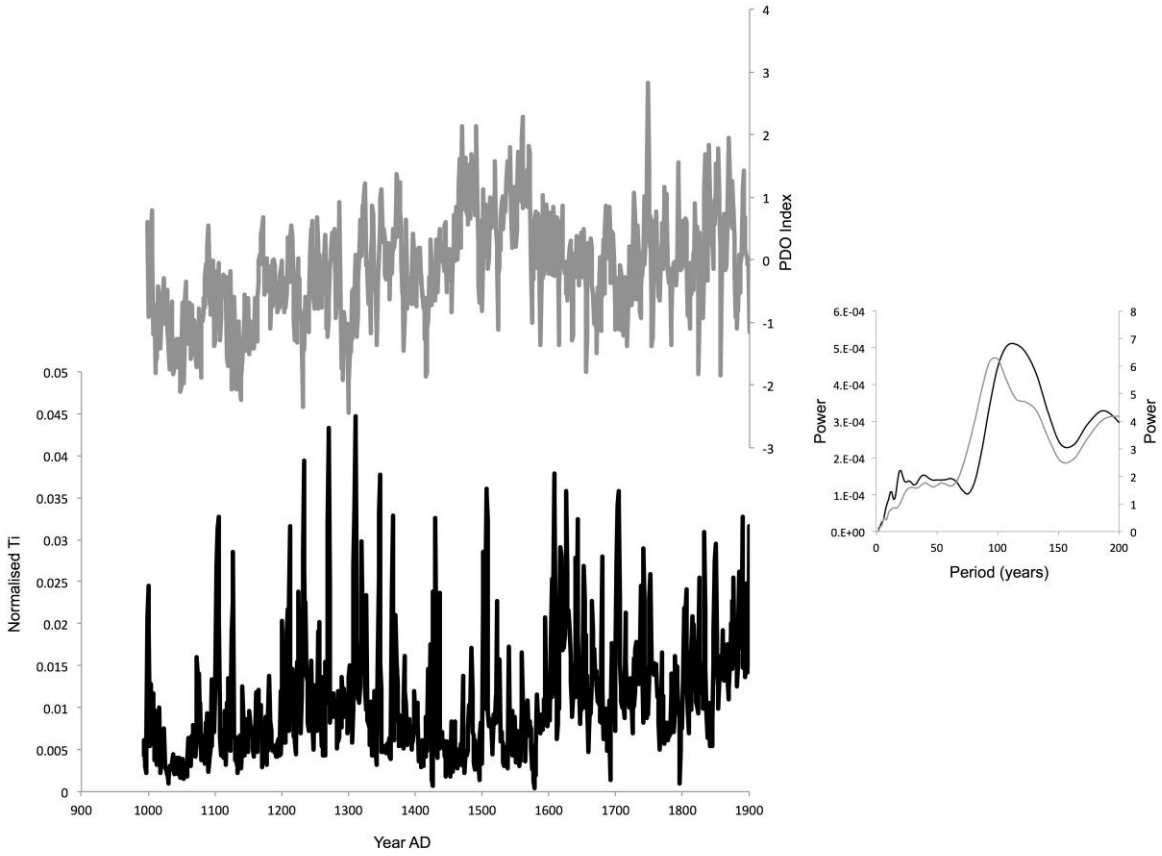

373

374 **Figure 4** Comparison of the Juanacatlán Ti record (black line) with the PDO reconstruction of
375 MacDonald and Case (2005) (grey line) between AD 993 and AD 1900. Also shown is a
376 comparison of the global wavelet power spectrum of the two time series, showing their
377 similarities; although none of the peaks in this plot are significant at the 95% confidence limit.

378

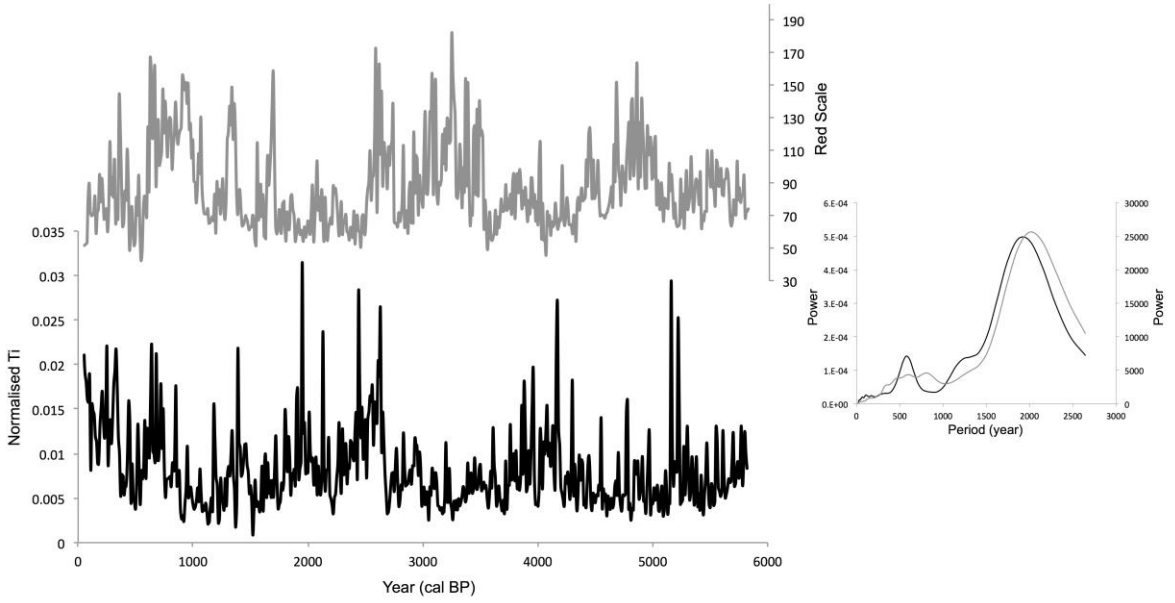

379
380

381 **Figure 5** Comparison of decadally smoothed Juanacatlán Ti and Pallcacocha red scale (Moy
382 et al., 2002) records through their common time period (50-5820 cal year BP). Also shown is
383 a comparison of the global wavelet power spectrum of the two time series, showing their
384 similarities. Only the c. 2000 year periodicities are significant at the 95% confidence limit
385 when using the decadally smoothed data.

386

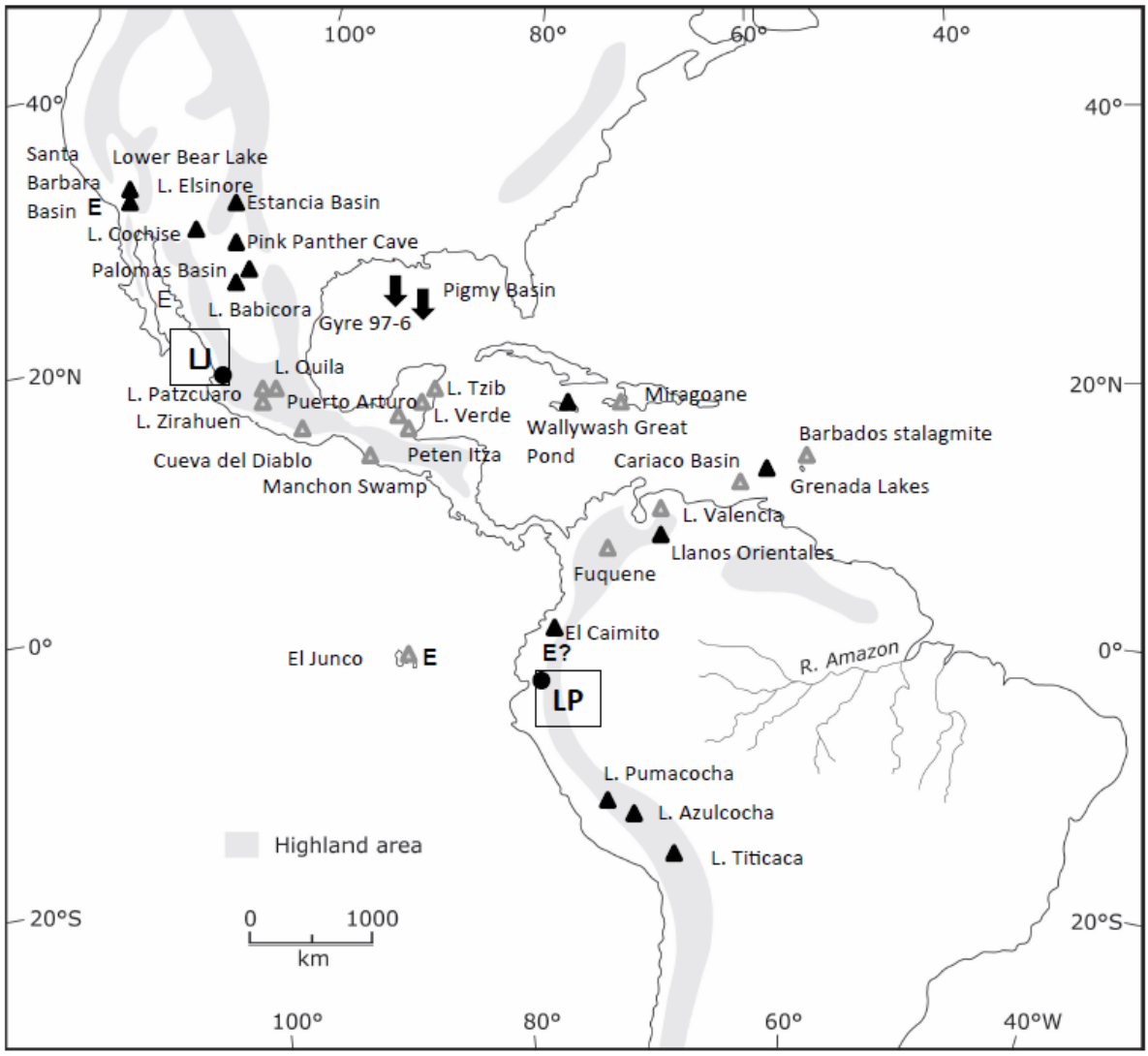

Figure 6 Spatial analysis of changes in climate conditions between 4 and 3 cal ka BP (sites and references are listed in Supplementary Table 2). LJ = Laguna de Juanacatlán, LP = Laguna Pallcacocha. Black triangles mark sites which get wetter through this time period, grey triangles sites which get drier. E indicates increasing ENSO activity. Downward pointing arrows indicate decreasing temperatures.